

Photochemistry of $(\text{OCS})_n^-$ cluster ions

Andrei Sanov, Sreela Nandi, Kenneth D. Jordan,^{a)} and W. Carl Lineberger
*JILA, National Institute of Standards and Technology and University of Colorado, and Department
 of Chemistry and Biochemistry, University of Colorado, Boulder, Colorado 80309-0440*

(Received 23 March 1998; accepted 16 April 1998)

We report the photochemistry of $(\text{OCS})_n^-$ cluster ions following 395 nm ($n=2-28$) and 790 nm ($n=2-4$) excitation. In marked contrast to $(\text{CO}_2)_n^-$, extensive bond breaking and rearrangement is observed. Three types of ionic products are identified: $\text{S}_2^-(\text{OCS})_k$, $\text{S}^-(\text{OCS})_k/\text{OCS}_2^-(\text{OCS})_{k-1}$, and $(\text{OCS})_k^-$. For $n < 16$, 395 nm dissociation is dominated by S_2^- -based fragments, supporting the theoretical prediction of a cluster core with a C_{2v} $(\text{OCS})_2^-$ dimer structure and covalent C-C and S-S bonds. A shift in the branching ratio in favor of S^- -based products is observed near $n=16$, consistent with an opening of the photodissociation pathway of OCS^- core-based clusters. These monomer-based cluster ions may coexist with the dimer-based clusters over a range of n , but electron detachment completely dominates photodissociation as long as their vertical electron detachment energy, increasing with addition of each solvent molecule, is less than the photon energy. An $(\text{OCS})_2^-$ conformer of C_2 symmetry with a covalent C-C bond is believed to be responsible for 790 nm dissociation of $(\text{OCS})_2^-$, yielding primarily OCS^- products. The yield of OCS^- , and thus the importance of the C_2 form of $(\text{OCS})_2^-$ cluster core, decreases with increasing n , perhaps due to more favorable solvation of the C_{2v} form of $(\text{OCS})_2^-$ and/or a solvent-induced increase in the rate of interconversion of conformers. The $(\text{OCS})_k^-$ products observed in 395 nm photodissociation of the larger ($n \geq 7$) clusters are attributed to photofragment caging. Formation and dissociation mechanisms of clusters with different core types are discussed. The photochemical properties of $(\text{OCS})_n^-$ are compared to those of the isovalent $(\text{CO}_2)_n^-$ and $(\text{CS}_2)_n^-$ species. © 1998 American Institute of Physics. [S0021-9606(98)01628-6]

I. INTRODUCTION

Studies of the isovalent $(\text{CO}_2)_n^-$, $(\text{OCS})_n^-$, and $(\text{CS}_2)_n^-$ clusters raise important issues of structure, solvation, and photochemical properties of cluster anions. While $(\text{CO}_2)_n^-$ and $(\text{CS}_2)_n^-$ have been the subject of several experimental¹⁻¹⁸ and theoretical^{3,8,19,20} studies, much less is known about $(\text{OCS})_n^-$. One fundamental question regarding these clusters is whether the excess electron is localized on a single monomer or shared between two (or more) monomer moieties.^{3-8,19-21} Photoelectron spectroscopic studies of $(\text{CO}_2)_n^-$ reveal sharp discontinuities in the vertical detachment energy (VDE) between $n=6$ and 7 and again between $n=13$ and 14.^{4,5} These discontinuities have been attributed to "core switching": a transformation of the charged cluster core from a delocalized-charge covalent $(\text{CO}_2)_2^-$ structure for $n < 6$ to CO_2^- for $7 \leq n \leq 13$, and back to $(\text{CO}_2)_2^-$ for $n > 13$. Fleischman and Jordan predicted, based on electronic structure calculations, that the global minimum of $(\text{CO}_2)_2^-$ corresponds to a D_{2d} symmetry structure with the excess charge equally partitioned between the two CO_2 moieties.¹⁹ The $(\text{CO}_2)_2^- \rightarrow \text{CO}_2^-$ core switching in $(\text{CO}_2)_n^-$ at $n=6$ was attributed^{4,5} to a more favorable solvation of the monomer anion, compared to the covalent dimer. The reverse switch occurring between $n=13$ and 14 accommodated⁵ the dimer-based "magic number" structure of $(\text{CO}_2)_{14}^-$.

Although electron photodetachment spectroscopy is an important tool in experimental determination of structure, complementary photodissociation studies are invaluable for full characterization of cluster structural and photochemical properties. For example, the similar 2.54 eV photoelectron spectra⁷ of $(\text{CS}_2)_2^-$ and CS_2^- were interpreted as implying that the observed $(\text{CS}_2)_2^-$ species is composed of a CS_2^- monomer "solvated" by a neutral CS_2 . However, recent photodetachment spectra⁶ of $(\text{CS}_2)_n^-$, $n=1-6$, obtained at a photon energy of 4.66 eV, indicated existence of covalent cyclic anions. Further evidence for cyclic $(\text{CS}_2)_2^-$ anions is provided by the observation of C_2S_2^- products in the photodissociation of $(\text{CS}_2)_n^-$, $n=2-4$ clusters.³ Finally, electronic structure calculations indicate that the lowest energy configuration of $(\text{CS}_2)_2^-$ has a covalent structure of C_{2v} symmetry.^{3,8,20}

In contrast, the only anionic products observed in UV photodissociation of $(\text{CO}_2)_n^-$ clusters were smaller $(\text{CO}_2)_k^-$ ions,¹ consistent with breaking only the weakest C-C bond in the covalent D_{2d} $(\text{CO}_2)_2^-$ cluster core.¹⁹ For 308 nm photons, the photodissociation sets in at $n=13$, with no photodissociation being observed for the $(\text{CO}_2)_{12}^-$ and smaller clusters.^{1,2} For $(\text{CO}_2)_{13}^-$, electron photodetachment accounts for about 80% of the photodestruction, but for $(\text{CO}_2)_{14}^-$ and the larger clusters, photodissociation dominates and occurs with a much larger yield than in $(\text{CO}_2)_{13}^-$.^{1,2} The sudden increase in the photodissociation yield at $n=14$ can be understood as follows. The $(\text{CO}_2)_n^-$, $n \leq 13$ clusters have

^{a)}Permanent address: Department of Chemistry, University of Pittsburgh, Pittsburgh, PA 15260.

VDEs below the 4.0 eV photon energy and electron photodetachment is the dominant photodestruction process. Switching of the core from CO_2^- to $(\text{CO}_2)_2^-$ at $n=14$ is accompanied by a sharp increase in the VDE [for $(\text{CO}_2)_{14}^-$, $\text{VDE} \approx 4.5$ eV],⁵ causing the electron detachment channel to close and leaving only the slower dissociation channel accessible. Although most $(\text{CO}_2)_{13}^-$ clusters are expected to have CO_2^- cores,⁵ a small fraction may have $(\text{CO}_2)_2^-$ cores, and these may be responsible for the observed^{1,2} photodissociation.

The greater stability of the $(\text{CO}_2)_2^-$ chromophore to photodetachment, compared to that of CO_2^- , is thus responsible for the 308 nm photodissociation of the $(\text{CO}_2)_n^-$, $n > 13$, clusters. Our theoretical studies^{20,22} of $(\text{OCS})_2^-$ and $(\text{CS}_2)_2^-$ have revealed that, as in $(\text{CO}_2)_2^-$, the most stable forms of the dimer anions are charge delocalized with VDEs much larger than those of the monomer anions solvated by one neutral molecule. Consequently, in all three systems, dimer-based clusters are expected to be more active in photodissociation at visible and near-UV wavelengths, compared to the monomer-based clusters, which are more susceptible to electron photodetachment. Both photoelectron spectroscopic and photodissociation studies are therefore necessary for adequate characterization of the photochemical properties of $(\text{CO}_2)_n^-$, $(\text{OCS})_n^-$, and $(\text{CS}_2)_n^-$.

We report the photodissociation dynamics of $(\text{OCS})_n^-$ cluster ions following 395 and 790 nm excitation. Using tandem time-of-flight (TOF) mass spectrometry, three types of ionic products are identified: $\text{S}_2^-(\text{OCS})_k$, $\text{S}^-(\text{OCS})_k/\text{OCS}_2^-(\text{OCS})_{k-1}$, and $(\text{OCS})_k^-$. This rich variety of photoproducts is consistent with the predicted²² existence of different $(\text{OCS})_n^-$ conformers. The abundance of disulfur compounds among the photodissociation products points toward a covalent ring structure of the dimer anion cluster core with C–C and S–S bonding. In the experiments at $\lambda = 395$ nm, the branching ratio shifts from favoring the S_2^- -based products to S^- -based products for cluster sizes $n \geq 16$. This is attributed to an opening of the photodissociation pathway of OCS^- -based clusters. These clusters may coexist with dimer-based clusters over a range of n and become active in photodissociation only when their VDEs, boosted by increasing solvation, exceed the photon energy. An $(\text{OCS})_2^-$ conformer of C_2 symmetry with a covalent C–C bond,²² analogous to the D_{2d} structure of $(\text{CO}_2)_2^-$,¹⁹ is believed to be responsible for the 790 nm dissociation of small $(\text{OCS})_n^-$ clusters yielding OCS^- products. The $(\text{OCS})_k^-$ photodissociation products from larger ($n \geq 7$) clusters observed following 395 nm excitation are attributed to photofragment caging.

Section II gives a brief description of the experiment, followed by the presentation of the experimental results in Sec. III. The discussion in Sec. IV addresses (1) structure and formation and dissociation mechanisms of covalent $(\text{OCS})_2^-$, and (2) the photodissociation channels for the $(\text{OCS})_n^-$ clusters. Concluding remarks are presented in Sec. V.

II. EXPERIMENT

A detailed description of the ion beam apparatus has been given elsewhere.²³ The $(\text{OCS})_n^-$ clusters are formed by attachment of slow secondary electrons to neutral OCS clusters in an electron-impact ionized pulsed (30-Hz) supersonic jet (5%–7% of OCS in Ar), with subsequent nucleation around the negatively charged core.²⁴ Initial cluster ion mass selection is achieved in a Wiley-McLaren TOF mass spectrometer, whereas mass analysis of ionic fragments is carried out utilizing a second, reflectron mass spectrometer tilted at a small angle with respect to the primary ion beam axis. The reflected fragments are detected with a microchannel plate (MCP) detector. The ion signal is amplified and sent to a transient digitizer for averaging and subsequent transfer to a computer. The precursor ion signal is simultaneously monitored with another MCP detector positioned directly behind the reflectron.

The fundamental or frequency-doubled output of a Quanta-Ray PDL-1 dye laser pumped with the second harmonic of a Quanta-Ray DCR-3 Nd:YAG laser was used as a source of the 790 and 395 nm radiation (<10-ns pulse duration; ~ 5 and 0.7 mJ/pulse at 790 and 395 nm, respectively). The fragment TOF mass spectra were recorded by averaging between 3000 and 10 000 laser shots. Subsequently, the mass spectrum peaks were integrated and the relative yields of different products were determined. The ionic products of metastable decay of precursor clusters were observed in the same way in the absence of laser radiation.

III. RESULTS

A. Parent distribution and metastable decay of $(\text{OCS})_n^-$ clusters

The distribution of $(\text{OCS})_n^-$ clusters in the primary ion beam displays no noticeable discontinuities over the cluster size range studied ($n = 2$ –28). The $(\text{OCS})_n^-$, $n \geq 3$ clusters exhibit metastable decay forming $(\text{OCS})_k^-$ ($2 \leq k < n$) fragments, but metastable decay of $(\text{OCS})_2^-$ is not observed. The OCS^- monomer anion is not observed in the primary ion beam, nor is it formed by metastable decay of larger clusters. These observations suggest that the $(\text{OCS})_n^-$ clusters, at least in the small n range, are best described as $(\text{OCS})_2^-(\text{OCS})_{n-2}$ with strongly bound dimer cores, and/or that OCS^- is unstable with respect to autodetachment [i.e., $EA(\text{OCS}) < 0$].

The number of OCS molecules lost by metastable decay is surprisingly large and cannot be attributed simply to the “temperature” of the cluster ion. For large $(\text{OCS})_n^-$ cluster ions ($n > 10$), metastable decay fragments corresponding to the loss of up to as many as six OCS molecules were observed. For comparison, metastable decay of $\text{I}_2^-(\text{OCS})_n^-$ clusters in the same ion beam is a very minor process.²⁵ One possible explanation for the enhanced decay of $(\text{OCS})_n^-$ is that some of these cluster ions are formed in metastable electronically excited states,²² and that the energy release into the cluster occurs slowly.

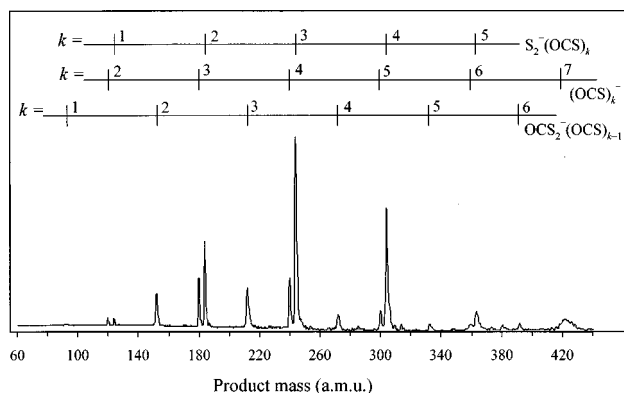


FIG. 1. Ionic fragment mass spectrum following 395 nm excitation of $(\text{OCS})_{12}^-$. The broadened $(\text{OCS})_7^-$ and $(\text{OCS})_6^-$ peaks correspond to metastable decay products that appear even without laser radiation.

B. Photodissociation of $(\text{OCS})_n^-$ clusters at 395 nm (3.14 eV)

A representative photofragment mass spectrum obtained by irradiating $(\text{OCS})_{12}^-$ at 395 nm is shown in Fig. 1. Three progressions of anionic photoproducts spaced by 60 a.m.u. (OCS mass) are clearly discernable. The corresponding product classes are $\text{S}_2^-(\text{OCS})_k$, $\text{S}^-(\text{OCS})_k$, and $(\text{OCS})_k^-$. All products observed in the photodissociation of $(\text{OCS})_n^-$ clusters ($n=2-28$) fall into one of these progressions.

Figure 2 displays the combined fractional yield of all products of each class (summed over k) versus the parent cluster size (n). Due to limited fragment mass resolution, the $(\text{OCS})_k^-$ and $\text{S}_2^-(\text{OCS})_{k-1}$ products, spaced by 4 a.m.u., could not be resolved for parent clusters with $n > 20$. The mass peaks corresponding to the third, $\text{S}^-(\text{OCS})_k$, channel separated from their neighbors by 28 a.m.u., are well resolved even for $n > 20$; the fractional yield of this channel was determined up to $n=28$.

The abundance of $\text{S}_2^-(\text{OCS})_k$ products over a wide range of parent $(\text{OCS})_n^-$ clusters suggests strong chemical interaction between sulfur atoms within the cluster, arguing in favor of a covalently bound $(\text{OCS})_2^-$ cluster core. Interestingly, photodissociation of $(\text{CS}_2)_n^-$, $n=2-4$ results in C_2S_2^- rather

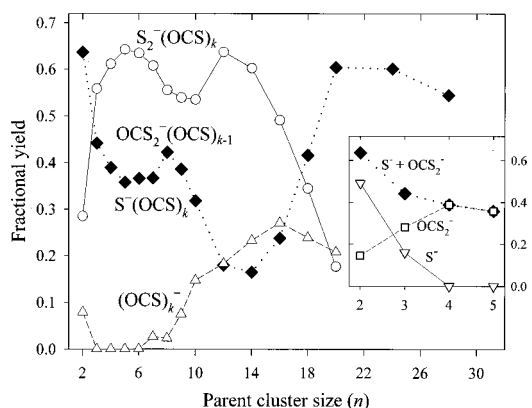


FIG. 2. Fractional yields of $\text{S}_2^-(\text{OCS})_k$, $\text{S}^-(\text{OCS})_k/\text{OCS}_2^-(\text{OCS})_{k-1}$, and $(\text{OCS})_k^-$ products (summed over k) in 395 nm dissociation of $(\text{OCS})_n^-$ clusters versus parent cluster size n . Inset illustrates the competition between S^- and OCS_2^- in the small n region.

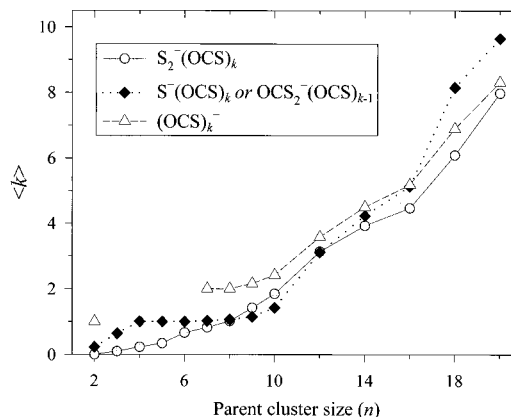


FIG. 3. Channel-specific average number of OCS moieties $\langle k \rangle$ in 395 nm photofragments of $(\text{OCS})_n^-$ as a function of the parent cluster size.

than S_2^- products.³ Also intriguing is the behavior of the $(\text{OCS})_k^-$ channel, which is a minor pathway for $(\text{OCS})_n^-$ clusters with $n=2$ and $n=7-20$ but is absent for $n=3-6$. This contrasts sharply with $(\text{CO}_2)_n^-$ photodissociation, where only $(\text{CO}_2)_k^-$, $k < n$ clusters were observed.¹ Other observations pertaining to the $(\text{OCS})_k^-$ channel include the following: (1) The photodissociation of $(\text{OCS})_2^-$ gives an OCS^- product (yield $\approx 8\%$), a species not present in the primary ion beam and not produced by metastable decay; (2) Between $n=7$ and 16, the yield of $(\text{OCS})_k^-$ fragments grows monotonically, as is characteristic of caging. For $n > 16$, the yield of $(\text{OCS})_k^-$ fragments decreases as does the importance of the $\text{S}_2^-(\text{OCS})_k$ channel. In contrast, the S^- channel becomes increasingly important for these larger clusters.

The $\text{S}^-(\text{OCS})_k$ products can also be ascribed to an $\text{OCS}_2^-(\text{OCS})_{k-1}$ structure, where the OCS_2^- core is a covalently bound anion, isovalent to CO_3^- or NO_3^- . Moreover, the $(\text{OCS})_k^-$ products can correspond to either OCS^- or $(\text{OCS})_2^-$ cores solvated by $(k-1)$ or $(k-2)$ OCS molecules, respectively. Figure 3, displaying the average numbers of OCS moieties $\langle k \rangle$ in photoproducts versus n , helps to discriminate between these possibilities. First, there exists a plateau at $\langle k \rangle = 1$ in the $\text{S}^-(\text{OCS})_k/\text{OCS}_2^-(\text{OCS})_{k-1}$ channel in the range of $n=4-8$. In fact, $\text{S}^-(\text{OCS})/\text{OCS}_2^-$ is the only fragment in this channel in 395 nm photodissociation of $(\text{OCS})_n^-$ with $n=4-6$. This indicates an extraordinary stability of the $k=1$ product, consistent with covalent OCS_2^- structure. The S^- product (i.e., $k=0$) is only observed in the photodissociation of $(\text{OCS})_2^-$ and $(\text{OCS})_3^-$ (see inset in Fig. 2). Second, when the $(\text{OCS})_k^-$ channel reopens at $n=7$, its $\langle k \rangle$ vs n dependence starts out along the $\langle k \rangle = 2$ line (see Fig. 3), suggesting that $(\text{OCS})_2^-$, not OCS^- , is the core of these products.

C. Photodissociation of $(\text{OCS})_n^-$ clusters at 790 nm (1.57 eV)

At 790 nm the photodissociation cross section decreases rapidly with cluster size. For $(\text{OCS})_3^-$, the cross section was estimated to be 3 to 4 times smaller than that for $(\text{OCS})_2^-$, while for $(\text{OCS})_4^-$ it drops by roughly another factor of 3 compared to $(\text{OCS})_3^-$. This trend continues for $(\text{OCS})_5^-$.

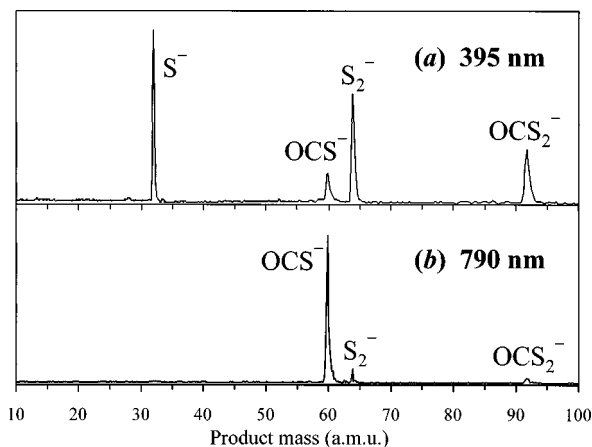


FIG. 4. Photofragment mass spectra obtained in photodissociation of $(\text{OCS})_2^-$ at (a) 395 nm and (b) 790 nm.

Figure 4 compares the photofragment mass spectra obtained in photodissociation of $(\text{OCS})_2^-$ at 395 and 790 nm. Figure 5 summarizes fractional yields of different 790 nm dissociation channels for $n=2-4$. At 790 nm, photodissociation of $(\text{OCS})_2^-$ results predominantly in production of OCS^- (see Fig. 4). For larger $(\text{OCS})_n^-$ clusters, the fractional yield of OCS^- decreases (see Fig. 5). No S^- is produced at 790 nm from either $(\text{OCS})_2^-$ or larger parent clusters. Combining this observation with the measurable yield of $\text{S}^-(\text{OCS})/\text{OCS}_2^-$ (see Fig. 5), we conclude as before that “ S^- -based” products with $k \geq 1$ have an OCS_2^- , rather than an S^- , ionic core.

IV. DISCUSSION

The following experimental observations suggest that, at least in the small n range, $(\text{OCS})_n^-$ clusters have strongly bound $(\text{OCS})_2^-$ cores: (1) The $(\text{OCS})_n^-$ distribution in the ion beam starts at $n=2$, and OCS^- is not formed either in the ion source or by metastable decay of $(\text{OCS})_n^-$ clusters, although it is observed as a photodissociation product; (2) Despite the metastable decay of $(\text{OCS})_n^-$ ($n \geq 3$), no decay is observed for $(\text{OCS})_2^-$; (3) $(\text{OCS})_2^-$ is a preferred 395 nm fragment in the $(\text{OCS})_k^-$ channel once it reopens at $n \geq 7$ (see Fig. 3).

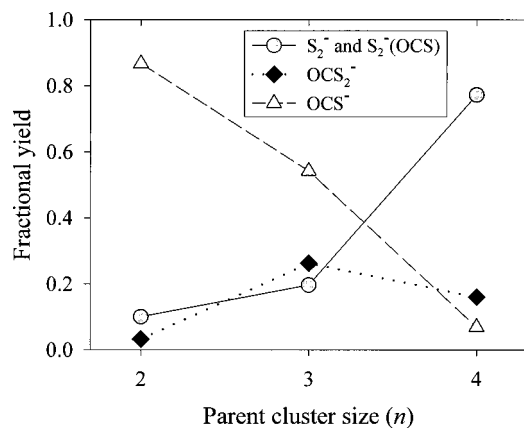


FIG. 5. Fractional yields of photofragments (summed over k) in 790 nm dissociation of $(\text{OCS})_n^-$ clusters versus parent cluster size n .

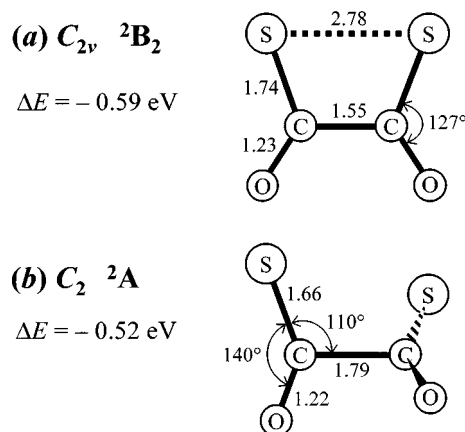


FIG. 6. Equilibrium geometries of $(\text{OCS})_2^-$ optimized at the MP2/6-31+G(d) level of theory. (a) C_{2v} structure corresponding to the global potential minimum of $(\text{OCS})_2^-$ with a 2B_2 symmetry electronic wave function. The C-C and S-S bond orders are 1 and 0.5, respectively. (b) C_2 structure corresponding to a 2A symmetry electronic wave function and a C-C bond order of 0.5. Bond lengths and angles are in Angstroms and degrees, respectively. Also shown are the energies ΔE relative to the $^1\text{OCS} + \text{OCS}^-$ asymptote (harmonic zero-point vibration energy corrections determined at the HF/6-31+G* level are included). Anion (a) can be viewed as arising from electron capture by covalently bound $(\text{OCS})_2$ (C_{2v} equilibrium geometry) with a doubly excited (with respect to van der Waals dimer) electronic configuration. Anion (b) arises from electron attachment to van der Waals dimer of OCS. Adapted from Ref. 22.

Moreover, the great abundance of $\text{S}_2^-(\text{OCS})_k$ photodissociation products suggests a strong chemical interaction between sulfur atoms within the cluster core.

A. $(\text{OCS})_2^-$ cluster core

1. $(\text{OCS})_2^-$ structure

We have investigated, at the MP2 level of theory the electronic structure of different conformers of the $(\text{OCS})_2^-$ anion.²² The two most stable covalently bound structures of $(\text{OCS})_2^-$ are reproduced in Fig. 6. The C_{2v} structure [Fig. 6(a)] corresponds to the global potential minimum of $(\text{OCS})_2^-$ with a 2B_2 symmetry electronic wave function and is predicted to lie ~ 0.6 eV below the $\text{OCS}^- + \text{OCS}$ dissociation limit (corrected for the harmonic zero-point vibrational energy). The 2.78 Å S-S bond length in the 2B_2 $(\text{OCS})_2^-$ anion corresponds to a bond order of 0.5. The calculations indicate that the 2B_2 $(\text{OCS})_2^-$ anion is both 0.3 eV more stable than the $\text{OCS}^-(\text{OCS})$ ion-molecule complex and ~ 0.1 eV more stable than the covalent C_2 form shown in Fig. 6(b).²² Given the small energy gap between the C_{2v} and C_2 forms of $(\text{OCS})_2^-$, coexistence of both conformers in the ion beam is quite possible. The C_2 form of $(\text{OCS})_2^-$ (2A electronic symmetry) is analogous to the most stable structure of $(\text{CO}_2)_2^-$ that has D_{2d} symmetry,¹⁹ the corresponding C_{2v} form of $(\text{CO}_2)_2^-$ lies higher in energy.²²

Figure 7 displays relevant potential energy curves of $(\text{OCS})_2^-$ and $(\text{OCS})_2$, constrained to C_{2v} symmetry.²² These curves were obtained by scanning the C-C distance, while relaxing all other degrees of freedom (subject to the C_{2v} constraint).²⁶ While the 2B_2 minimum in Fig. 7 is the global minimum for $(\text{OCS})_2^-$, the 2A_1 C_{2v} minimum is a saddle

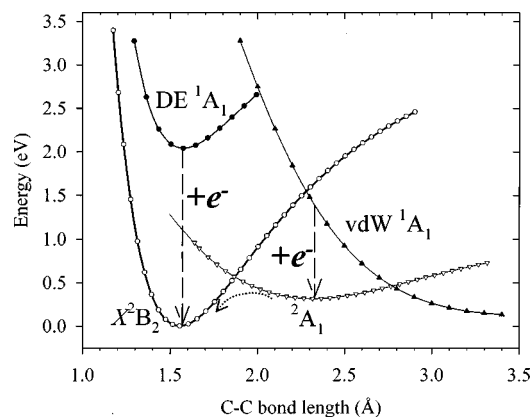


FIG. 7. Potential energy scans of relevant low-lying electronic states of $(\text{OCS})_2^-$ and $(\text{OCS})_2$, constrained to C_{2v} symmetry, with respect to C–C bond length, while relaxing all other degrees of freedom (subject to C_{2v} constraint). vdW 1A_1 denotes the van der Waals state of $(\text{OCS})_2$; DE 1A_1 corresponds to covalently bound cyclic $(\text{OCS})_2$, with electronic configuration doubly excited with respect to van der Waals complex. Down arrows indicate formation of the 2B_2 and 2A_1 dimer anions by direct electron attachment to DE 1A_1 and vdW 1A_1 $(\text{OCS})_2$, respectively. Curved dashed arrow indicates the formation of 2B_2 $(\text{OCS})_2^-$ by internal conversion from the 2A_1 state, following electron capture by van der Waals $(\text{OCS})_2$. Results of MP2/6-31+G(d) calculations adapted from Ref. 22.

point, unstable to twisting to the C_2 geometry shown in Fig. 6(b). There are several other low-lying states of $(\text{OCS})_2^-$, not shown in Fig. 7,²² which could be responsible for the observed metastable decay of $(\text{OCS})_n^-$, $n > 2$.

2. $C_{2v}(^2B_2)$ $(\text{OCS})_2^-$ formation and dissociation mechanisms

Electron attachment to a van der Waals cluster of OCS could directly form the $C_2(^2A)$ form of $(\text{OCS})_2^-$, but the electronic configuration^{20,22} of the 2B_2 C_{2v} anion necessitates a more elaborate formation mechanism. This anion has an electronic configuration consistent with electron attachment to a neutral dimer with an electronic configuration doubly excited (DE) with respect to that of the van der Waals dimer (vdW 1A_1 in Fig. 7).^{20,22} This doubly excited, covalently bound $(\text{OCS})_2$ molecule has a C_{2v} equilibrium geometry and is chemically analogous to elusive dioxetanedi-one (C_2O_4).²⁷ It can be viewed as arising from association of two $^3A'$ excited OCS molecules into a singlet dimer. Although the 2B_2 C_{2v} anion could result from electron capture by the metastable doubly excited neutral dimers, which could be present in our source, the dominant formation mechanism of $C_{2v}(^2B_2)$ $(\text{OCS})_2^-$ is likely to involve electron attachment to van der Waals clusters, followed by internal conversion to the $C_{2v}(^2B_2)$ state (see Fig. 7).

The transition dipole moments connecting the X^2B_2 and low-lying excited states of $(\text{OCS})_2^-$, calculated²⁶ using the CIS/6-31+G(d) method,²⁸ suggest that the strongest transition is $^2A_1 \leftarrow ^2B_2$, whose oscillator strength of 0.24 is over 2 orders of magnitude greater than those of the other low-lying transitions. Although this makes the $^2A_1 \leftarrow ^2B_2$ transition the prime candidate for initiating the observed photochemistry, direct dissociation on the 2A_1 surface cannot account for S_2^- -based products, a consequence of the nonbonding nature

of S–S interaction on this surface.^{20,22} Therefore, dissociation is likely to rely on nonadiabatic mixing of the optically bright 2A_1 state with other low-lying electronic states.

B. Dissociation pathways of $(\text{OCS})_n^-$ clusters, $2 \leq n < 16$

1. Photochemistries of OCS^- , $\text{C}_2(\text{OCS})_2^-$, and $\text{C}_{2v}(\text{OCS})_2^-$ cluster cores

Unlike S_2^- -based products, S^- could arise from photodissociation of OCS^- -based clusters. For small n , clusters with OCS^- cores are unlikely to be important, because OCS^- monomers are not observed in the ion beam and the $\text{OCS}^-(\text{OCS})$ ion-molecule complex is predicted to be 0.3 eV less stable than the covalent C_{2v} dimer.²² Moreover, electron detachment would likely be the only photodestruction pathway of small OCS^- -based clusters, because the VDE of these clusters is small compared to the photon energy [e.g., the predicted VDE of $\text{OCS}^-(\text{OCS})$ is 1.2 eV].²² A complementary 790 nm pump–probe experiment on $(\text{OCS})_2^-$ did not reveal any S^- signal resulting from photodissociation of OCS^- , the major photoproduct of $(\text{OCS})_2^-$ at 790 nm. Experiments on $(\text{CO}_2)_n^-$ clusters^{1,2,4,5} have also shown that dissociation cannot compete with electron detachment if the photon energy exceeds the anion VDE and that $(\text{CO}_2)_n^-$ clusters with CO_2^- cores are inactive in UV photodissociation.

Coexistence of the C_2 and C_{2v} covalent forms of $(\text{OCS})_2^-$ is likely because of their small energy separation. Due to the large (3.35 eV) VDE predicted²² for the $C_{2v}(^2B_2)$ $(\text{OCS})_2^-$ anion, photodissociation is expected to be the major photodestruction pathway for $(\text{OCS})_n^-$ clusters with covalent C_{2v} cores at both 395 and 790 nm. The calculated VDE of $C_2(\text{OCS})_2^-$ is 2.9 eV;²² it is expected to increase with each additional OCS molecule, gradually shifting the 395 nm (3.14 eV) photodestruction balance in favor of dissociation. Since the C–C bond is the weakest in the $C_2(\text{OCS})_2^-$ anion, OCS^- is likely to be the major photodissociation product. The decrease in OCS^- yield with increasing n for small $(\text{OCS})_n^-$ clusters (at both 395 and 790 nm) hints at the decreasing importance of the C_2 dimer-based $(\text{OCS})_n^-$ clusters, possibly due to more favorable solvation of $C_{2v}(\text{OCS})_2^-$ and/or a solvent-induced increase in the rate of internal conversion from the C_2 2A to the C_{2v} 2B_2 state of the $(\text{OCS})_2^-$ core.

2. $S_2^-(\text{OCS})_k$ products

This channel is the main experimental indication of a covalent-ring dimer structure of the cluster core. It is intriguing that photodissociation of small $(\text{CS}_2)_n^-$ clusters yields C_2S_2^- products,³ while photodissociation of the $(\text{OCS})_n^-$ clusters results in S_2^- -based products. Figure 8 presents a diagram, based on results of MP2/6-31+G(d) calculations,²⁶ which highlights the energetics of $C_{2v}(\text{OCS})_2^-$ dissociation. The alternative $\text{C}_2\text{O}_2^- + \text{S}_2$ channel, analogous to the $\text{C}_2\text{S}_2^- + \text{S}_2$ channel in $(\text{CS}_2)_2^-$, lies 2.4 eV above the $2\text{CO} + \text{S}_2^-$ pathway and is energetically inaccessible at the 395 nm photon energy.

In the case of larger $(\text{OCS})_n^-$ clusters, some of the S_2^- -based products may result from secondary chemical re-

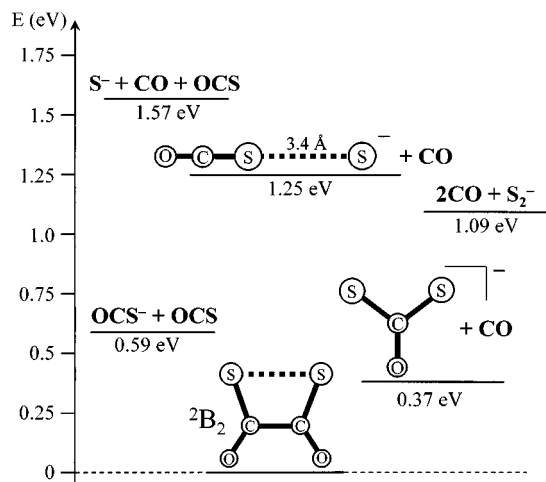


FIG. 8. Energetics of 2B_2 $(\text{OCS})_2^-$ dissociation, based on results of MP2/6-31+G(d) calculations. Harmonic zero-point vibrational energy corrections, derived from HF/6-31+G(d) frequency calculations, are included.

actions of S^- , produced as a primary photoproduct, with solvent OCS. An analogous photoinduced chemical reaction producing S_2 has been observed in $(\text{OCS})_n$ van der Waals clusters.²⁹

3. $\text{OCS}_2^-(\text{OCS})_{k-1}$ and $\text{S}^-(\text{OCS})_k$ products

The calculated threshold for production of S^- from C_{2v} $(\text{OCS})_2^-$, 1.57 eV, is very close to the 790 nm photon energy. In contrast, the $\text{OCS}_2^- + \text{CO}$ product channel is predicted to lie only 0.37 eV above the 2B_2 ground state of $(\text{OCS})_2^-$ (see Fig. 8). Experimental evidence in favor of the $\text{OCS}_2^-(\text{OCS})_{k-1}$ structure rather than the $\text{S}^-(\text{OCS})_k$ structure includes the following: (1) preferential formation of OCS_2^- (i.e., $k=1$) over a broad range of parent cluster size n , as seen in Fig. 3, and (2) an observation of OCS_2^- in 790 nm dissociation of $(\text{OCS})_n^-$, and the absence of an S^- product.

In order for OCS_2^- to be formed from the C_{2v} $(\text{OCS})_2^-$ species, the C–C bond and one of the C–S bonds must be fractured, leaving the remaining OCS group and the S atom in a relative arrangement consistent with the OCS_2^- structure (see Fig. 8). However, at the wavelengths used the OCS_2^- complex would be unstable to breakup to either $\text{S}^- + \text{OCS}$ or $\text{S}_2^- + \text{CO}$. In the absence of solvent molecules, the excess energy of OCS_2^- can only be transferred to the CO fragment; in the trimer and larger $(\text{OCS})_n^-$ clusters stabilization can occur via ejection of solvent molecules.

Further insight into the OCS_2^- breakup dynamics is provided by our brief study of OCS_2^- photodissociation.³⁰ At 395 nm, the only observed ionic fragment is S^- , but both S^- and S_2^- are produced in equal yield at 790 nm. Therefore, S^- is likely the dominant breakup product of an isolated highly excited OCS_2^- intermediate. Competition between S^- and S_2^- fragments may ensue as the excess energy is partially transferred to the solvent. A larger solvent shell may stabilize the OCS_2^- intermediate as a final product. This mechanism is consistent with the disappearance of S^- products at 395 nm for $n > 3$, accompanied by a rise in the S_2^- and OCS_2^- yields (see Fig. 2).

4. $(\text{OCS})_k^-$ products

The $(\text{OCS})_k^-$, $k \geq 2$ products in $(\text{OCS})_n^-$, $n \geq 7$ dissociation at 395 nm could derive from caging of photofragments. However, OCS^- observed in 395 nm dissociation of $(\text{OCS})_2^-$ and in dissociation of small $(\text{OCS})_n^-$ clusters at 790 nm must derive from dissociation of the $(\text{OCS})_2^-$ cluster core. The absence of $(\text{OCS})_k^-$ products at 395 nm in the parent size range $n=3-6$, where $\text{S}_2^-(\text{OCS})_k$ is the dominant dissociation channel, suggests that OCS^- is not produced in dissociation of $C_{2v}({}^2B_2)$ $(\text{OCS})_2^-$ at this wavelength. The most likely origin of OCS^- in 790-nm dissociation of $(\text{OCS})_n^-$, $n=2-4$, is from the C_2 form of $(\text{OCS})_2^-$ cluster core, while the S_2^- and OCS_2^- products derive from clusters with the C_{2v} dimer core. The population of $(\text{OCS})_n^-$ clusters with C_2 $(\text{OCS})_2^-$ cores in the ion beam apparently decreases with n , leading to a decrease in the total 790 nm dissociation yield, manifested mainly as a drop in the OCS^- channel.

C. Photochemistry of larger $(\text{OCS})_n^-$ clusters ($n \geq 16$): Closure of the photodetachment channel or core switching?

As has been demonstrated for $(\text{CO}_2)_n^-$ clusters,^{4,5} solvation can shift the energetics in favor of a different type of cluster core. More favorable solvation of the smaller (compared to the dimer) monomer anion may lower the overall energy of OCS^- -based clusters and result in their coexistence with $(\text{OCS})_2^-$ -based clusters over a range of n with gradual population shift in favor of the former. On the other hand, the monomer-based clusters remain inactive in photodissociation until solvation boosts the VDE above the photon energy, closing the electron detachment channel in favor of dissociation. A combination of these effects is likely responsible for the change in the $(\text{OCS})_n^-$ fragmentation pattern around $n=16$, manifested as an abrupt decrease in the yield of S_2^- -based products, and a rise in $\text{S}^-(\text{OCS})_k$ or $\text{OCS}_2^-(\text{OCS})_{k-1}$ fragments (see Fig. 2).

Given the calculated²² 1.2-eV VDE for the $\text{OCS}^-(\text{OCS})$ ion-molecule complex and assuming that each additional solvent molecule increases the VDE by ~ 0.2 eV, we find that the VDE of OCS^- -based $(\text{OCS})_n^-$ clusters should exceed the 395-nm photon energy (3.14 eV) for $n > 12$. Therefore, the observed shift in fragmentation pattern is not necessarily indicative of $(\text{OCS})_2^- \rightarrow \text{OCS}^-$ core switching occurring near $n=16$; rather, it may signify a closing of the electron detachment channel and an opening of the dissociation pathway for the OCS^- -based clusters. In the $(\text{CO}_2)_n^-$ clusters conformer coexistence is apparently limited to a single cluster size.^{4,5} However, the present results suggest that for $(\text{OCS})_n^-$ different structural forms of the clusters can coexist over a broad range of n .

V. CONCLUSIONS

In summary, we have investigated the photodissociation of $(\text{OCS})_n^-$ clusters at 395 nm ($n=2-28$) and 790 nm ($n=2-4$). Three classes of ionic photoproducts are identified: $\text{S}_2^-(\text{OCS})_k$, $\text{S}^-(\text{OCS})_k/\text{OCS}_2^-(\text{OCS})_{k-1}$, and $(\text{OCS})_k^-$. Such a rich variety of products is in sharp contrast with the photodissociation of isovalent $(\text{CO}_2)_n^-$, which yields exclu-

sively $(\text{CO}_2)_k^-$ ($k < n$) fragments.^{1,2} The S_2^- -based fragments represent the dominant 395 nm dissociation pathway of $(\text{OCS})_n^-$, $n=3-16$, strongly supporting the theoretical prediction²² of a covalent cyclic structure of $(\text{OCS})_2^-$ cluster core.

The OCS^- produced in $(\text{OCS})_n^-$ ($n=2-4$) dissociation at 790 nm likely results from the C_2 covalent form of $(\text{OCS})_2^-$ cluster core, analogous in electronic structure and geometry to the D_{2d} dimer¹⁹ core of $(\text{CO}_2)_n^-$ clusters ($2 \leq n < 7$ and $n > 13$).^{4,5} The importance of the C_2 form of the $(\text{OCS})_2^-$ cluster core decreases with cluster size, probably due to more favorable solvation of C_{2v} $(\text{OCS})_2^-$ and/or a solvent-induced increase in the rate of internal conversion from the C_2 2A to the C_{2v} 2B_2 form of the $(\text{OCS})_2^-$ core. The $(\text{OCS})_k^-$ products of larger $(\text{OCS})_n^-$ clusters ($n \geq 7$) observed upon 395 nm irradiation are attributed to photofragment caging.

For larger clusters, more favorable solvation of the monomer anion results in coexistence of the OCS^- and $(\text{OCS})_2^-$ -based $(\text{OCS})_n^-$ clusters over a range of n with a gradual population shift in favor of the former. The monomer-based clusters remain inactive in photodissociation as long as the VDE is below the photon energy. The shift in the fragmentation pattern in favor of the S^- -based products occurring around $n=16$ signifies the solvent-induced increase in the VDE, closing the detachment pathway and opening the dissociation channel of the OCS^- -based clusters. Photoelectron spectroscopic studies, currently under way in our laboratory, should yield more complete understanding of structure and photochemistry of $(\text{OCS})_n^-$ cluster ions.

ACKNOWLEDGMENTS

This work is supported by the National Science Foundation (Grant Nos. CHE97-03486 and PHY95-12150) and the Air Force Office of Scientific Research (AASERT program). K.D.J. acknowledges the support of a Visiting Fellowship at JILA.

¹M. L. Alexander, M. A. Johnson, N. E. Levinger, and W. C. Lineberger, *Phys. Rev. Lett.* **57**, 976 (1986).

²M. L. Alexander, Ph.D. thesis, University of Colorado at Boulder, 1987.

³T. Maeyama, T. Oikawa, T. Tsumura, and N. Mikami, *J. Chem. Phys.* **108**, 1368 (1998).

⁴M. J. DeLuca, B. Niu, and M. A. Johnson, *J. Chem. Phys.* **88**, 5857 (1988).

⁵T. Tsukuda, M. A. Johnson, and T. Nagata, *Chem. Phys. Lett.* **268**, 429 (1997).

⁶T. Tsukuda, T. Hirose, and T. Nagata, *Chem. Phys. Lett.* **279**, 179 (1997).

⁷K. H. Bowen and J. G. Eaton, in *The Structure of Small Molecules and Ions*, edited by R. Naaman and Z. Vager (Plenum, New York, 1988), p. 147; C. B. Freidhoff, Ph.D. dissertation, Johns Hopkins University, 1987.

⁸K. Hiraoka, S. Fujimaki, G. Aruga, and S. Yamabe, *J. Physiol. (London)* **98**, 1802 (1994).

⁹C. E. Klots and R. N. Compton, *J. Chem. Phys.* **67**, 1779 (1977).

¹⁰C. E. Klots and R. N. Compton, *J. Chem. Phys.* **69**, 1636 (1978).

¹¹M. Knapp, D. Kreisle, O. Echt, K. Sattler, and E. Recknagel, *Surf. Sci.* **156**, 313 (1985).

¹²M. Knapp, O. Echt, D. Kreisle, T. D. Mark, and E. Recknagel, *Chem. Phys. Lett.* **126**, 225 (1986).

¹³A. Stamatovic, K. Leiter, W. Ritter, K. Stephan, and T. D. Mark, *J. Chem. Phys.* **83**, 2942 (1985).

¹⁴H. Langosh and H. Haberland, *Z. Phys. D* **2**, 243 (1986).

¹⁵T. Kondow and K. Mitsuke, *J. Chem. Phys.* **83**, 2612 (1985).

¹⁶T. Kondow, *J. Phys. Chem.* **91**, 1307 (1987).

¹⁷F. Misaizu, K. Mitsuke, T. Kondow, and K. Kuchitsu, *J. Chem. Phys.* **94**, 243 (1991).

¹⁸T. Kraft, M. W. Ruf, and H. Hotop, *Z. Phys. D* **14**, 179 (1989).

¹⁹S. H. Fleischman and K. D. Jordan, *J. Phys. Chem.* **91**, 1300 (1987).

²⁰A. Sanov, W. C. Lineberger, and K. D. Jordan, *J. Phys. Chem. A* **102**, 2509 (1998).

²¹A. W. Castleman and K. H. Bowen, *J. Phys. Chem.* **100**, 12 911 (1996).

²²A. Sanov, W. C. Lineberger, and K. D. Jordan (in preparation).

²³M. E. Nadal, P. D. Kleiber, and W. C. Lineberger, *J. Chem. Phys.* **105**, 504 (1996).

²⁴M. A. Johnson and W. C. Lineberger, in *Techniques for the Study of Ion Molecule Reactions*, edited by J. M. Farrar and J. W. Saunders (Wiley, New York, 1988), p. 591.

²⁵S. Nandi, A. Sanov, and W. C. Lineberger (in preparation).

²⁶M. J. Frisch, G. W. Trucks, H. B. Schlegel, P. M. W. Gill, B. G. Johnson, M. A. Robb, J. R. Cheeseman, T. Kieth, G. A. Petersson, J. A. Montgomery, K. Raghavachari, M. A. Al-Laham, V. G. Zakrewski, J. V. Ortiz, J. B. Foresman, J. Cioslowski, B. B. Stefanov, A. Nanayakkara, M. Challacombe, C. Y. Peng, P. Y. Ayala, W. Chen, M. W. Wong, J. L. Andres, E. S. Replogle, R. Gomperts, R. L. Martin, D. J. Fox, J. S. Binkley, D. J. Defrees, J. Baker, J. P. Stewart, M. Head-Gordon, C. Gonzalez, and J. A. Pople, *GAUSSIAN 94*, Rev. E.1 (Gaussian, Inc., Pittsburgh, PA, 1994).

²⁷M. M. Rauhut, L. J. Bollyky, B. G. Roberts, M. Loy, R. H. Whitman, A. V. Iannotta, A. M. Semsel, and R. A. Clarke, *J. Am. Chem. Soc.* **89**, 6515 (1967).

²⁸J. B. Foresman, M. Head-Gordon, P. J. A., and M. J. Frisch, *J. Phys. Chem.* **96**, 135 (1992).

²⁹N. Sivakumar, G. E. Hall, P. L. Houston, J. W. Hepburn, and I. Burak, *J. Chem. Phys.* **88**, 3692 (1988).

³⁰A. Sanov and W. C. Lineberger, unpublished results.